Oil & Gas Science and Technology – Rev. IFP, Vol. 60 (2005), No. 2, pp. 275-285

IFP International Workshop
Rencontres scientifiques de l'IFP

Gas-Water-Rock Interactions ... / Interactions gaz-eau-roche ...

Thermodynamic Analysis of Organic/Inorganic Reactions Involving Sulfur: Implications for the Sequestration of H_2S in Carbonate Reservoirs

L. Richard[1,2], N. Neuville[1], J. Sterpenich[2], E. Perfetti[1,2] and J.C. Lacharpagne[3]

1 Université Henri-Poincaré, Département des sciences de la Terre, 54506 Vandœuvre-lès-Nancy Cedex - France
2 Géologie et gestion des ressources minérales et énergétiques, UMR 7566 G2R, 54506 Vandœuvre-lès-Nancy Cedex - France
3 Total, CSTJF, avenue Larribau, 64018 Pau Cedex - France
e-mails: laurent.richard@g2r.uhp-nancy.fr - nadineneuville@yahoo.fr - jerome.sterpenich@g2r.uhp-nancy.fr - erwan.perfetti@g2r.uhp-nancy.fr jean-claude.lacharpagne@total.com

Résumé — Étude thermodynamique des réactions organiques/inorganiques du soufre : implications pour la séquestration de H_2S dans des réservoirs carbonatés — Les interactions eaux-gaz-roches-hydrocarbures impliquant le soufre dans des réservoirs pétroliers carbonatés sont analysées d'un point de vue thermodynamique. Des calculs d'équilibre minéraux-solutions indiquent que les eaux de formation de réservoirs carbonatés du Bassin parisien, du bassin de l'Alberta et de la mer du Nord sont en équilibre avec la calcite et la dolomite, mais qu'elles ne le sont pas avec l'anhydrite. Une augmentation de l'activité du sulfure d'hydrogène dans la phase aqueuse ($a_{H_2S_{(aq)}}$) favorise la formation de soufre élémentaire, laquelle constitue une réaction de séquestration possible pour H_2S.

Il est également suggéré que les fortes pressions partielles de H_2S associées à une réduction thermochimique des sulfates dans des réservoirs carbonatés pourraient être contrôlées par des équilibres métastables entre hydrocarbures, composés organiques soufrés, soufre élémentaire et H_2S gazeux. Ces pressions partielles de H_2S sont de 4 à 6 ordres de grandeur plus élevées que celles observées dans les réservoirs clastiques et pour lesquelles un contrôle par des équilibres entre H_2S, pyrite et carbonates ferrifères a été proposé. Selon les rapports H/C des hydrocarbures et des composés organiques soufrés, H_2S peut être soit produit, soit consommé au cours des réactions de sulfurisation des huiles dans les réservoirs carbonatés.

Abstract* — *Thermodynamic Analysis of Organic/Inorganic Reactions Involving Sulfur: Implications for the Sequestration of H_2S in Carbonate Reservoirs — *A thermodynamic analysis has been made of water-gas-rock-hydrocarbon interactions involving sulfur in carbonate reservoirs. Mineral-solution equilibria calculations indicate that formation waters produced from carbonate reservoirs at temperatures between 40°C and 160°C in the Paris Basin, Alberta Basin, and the North Sea are saturated with respect to calcite and dolomite, but undersaturated with respect to anhydrite. The calculations also suggest that increasing the activity of dissolved H_2S ($a_{H_2S_{(aq)}}$) in the reservoirs favors the formation of elemental sulfur, which constitutes a potential sequestration reaction for H_2S.*

It is also shown that high partial pressures of H_2S generated by thermochemical sulfate reduction in carbonate reservoirs may be controlled by metastable equilibrium states between hydrocarbons, organic

sulfur compounds, elemental sulfur, and H_2S at partial pressures which are 4 to 6 orders of magnitude higher than in clastic reservoirs where the H_2S partial pressures are controlled by pyrite and iron carbonates. Depending on the H/C ratios of the hydrocarbons and organic sulfur compounds, H_2S may be consumed or produced as a result of petroleum sulfurization reactions in carbonate reservoirs.

INTRODUCTION

Carbon dioxide (CO_2) and hydrogen sulfide (H_2S) are both gases of environmental concern. The constant increase in the concentration of atmospheric CO_2 with increasing industrial activity over the last 150 years is a major cause in today's climate change [1], and the sequestration of CO_2 through dissolution in formation waters and subsequent neutralization of aqueous carbonic acid by rock-forming minerals has been proposed as a short-term means to reduce the level of CO_2 released into the atmosphere [2]. The conversion into elemental sulfur of the hydrogen sulfide which is commonly produced along with CO_2 from sour gas-containing reservoirs is sometimes of doubtful economic interest. A possible alternative is the reinjection of CO_2-H_2S mixtures in depleted hydrocarbon reservoirs [3-5]. Such a reinjection of CO_2-H_2S mixtures in gas-water-rock-hydrocarbon environments will result in thermal and chemical perturbations, which will be manifested by mass transfers among the gas phase, formation waters, liquid hydrocarbons, and rock-forming minerals. The transformations resulting from the injection may include, among others, a drastic decrease in the pH of the aqueous fluids, the dissolution of carbonates and sulfates, the precipitation of sulfides and elemental sulfur, and the formation of organic sulfur compounds through sulfurization of the residual oil. Following the metastable equilibrium approach pioneered by Helgeson *et al.* [6], we present a thermodynamic analysis of the equilibrium relations between minerals, aqueous fluids, hydrocarbons, and hydrogen sulfide in carbonate reservoirs.

1 THERMODYNAMIC RELATIONS

The equilibrium constant $K_{r,T,P}$ of the *r*th reaction at a given temperature *T* and pressure *P* is given by:

$$K_{r,T,P} = \exp\ \frac{-\Delta G_r^\circ}{RT} \tag{1}$$

where ΔG_r^o is the standard molal Gibbs free energy of the *r*th reaction, *R* stands for the gas constant (1.9872 cal $mol^{-1}K^{-1}$), and *T* and *P* denote the absolute temperature and total pressure expressed in Kelvin and bar, respectively. The standard molal Gibbs free energy of the *r*th reaction is defined by:

$$\Delta G_r^\circ = \sum_i n_{i,r} \Delta G_i^\circ \tag{2}$$

where $n_{i,r}$ represents the reaction coefficient of the *i*th species in the *r*th reaction, which is negative for reactants and positive for products, and ΔG_i^o stands for the apparent standard molal Gibbs free energy of formation of the *i*th species at the temperature *T* and pressure *P* of interest. Omitting the *i* subscript for simplicity, the latter property can be calculated from [7]:

$$\Delta G_i^\circ \equiv \Delta G^\circ = \Delta G_f^\circ + (G_{T,P}^\circ - G_{T_r,P_r}^\circ) \tag{3}$$

where ΔG_f^o stands for the standard molal Gibbs free energy of formation at the reference temperature and pressure of 25°C and 1 bar, and $(G_{T,P}^o - G_{T_r,P_r}^o)$ represents the difference in the standard molal Gibbs free energy of the *i*th species at the temperature and pressure of interest, and that at the reference temperature and pressure (T_r and P_r). In accord with [6], the standard state adopted for minerals, liquid H_2O, and liquid hydrocarbons and organic sulfur compounds in petroleum is one of unit activity of the thermodynamic components of stoichiometric minerals and pure liquids at any temperature and pressure. The standard state for aqueous species other than H_2O is one of unit activity of the species in a hypothetical one molal solution referenced to infinite dilution at any pressure and temperature. The standard state for gases is specified as unit fugacity of the pure hypothetical ideal gas at 1 bar and any temperature.

The parenthetical term in Equation (3) is evaluated by integrating in temperature and pressure the expression:

$$G_{T,P}^\circ - G_{T_r,P_r}^\circ = -S_{T_r,P_r}^\circ (T - T_r) + \int_{T_r}^{T} C_{P_r}^\circ dT - T\int_{T_r}^{T} C_{P_r}^\circ d\ln T + \int_{P_r}^{P} V^\circ dP \tag{4}$$

where S_{T_r,P_r}^o stands for the standard molal entropy of the species at 25°C and 1 bar, $C_{P_r}^o$ denotes the standard molal heat capacity of the species at the reference pressure of 1 bar, and V^o represents the standard molal volume of the species at the temperature and pressure of interest. The temperature dependence above 298.15 K of the standard molal heat capacity at 1 bar of minerals, inorganic gases, and organic liquids can be represented by the Maier-Kelley equation [7-9], which is written as [10]:

$$C_{P_r}^\circ = a + bT + cT^{-2} \tag{5}$$

where *a*, *b*, and *c* stand for temperature-independent coefficients. Consideration of compressibility and thermal

expansivity data indicates that the standard molal volume of minerals is insensitive to changes in temperature and pressure for the conditions encountered in sedimentary basins [7]. Although the standard molal volumes of organic liquids are much more dependent on temperature and pressure than those of minerals, experimental data indicate that the effects of simultaneously increasing temperature and pressure tend to compensate along typical sedimentary basin geotherms [11]. Consequently, the last integral in Equation (4) reduces to:

$$\int_{P_r}^{P} V^{\circ} dP = V^{\circ}_{T_r,P_r} (P - P_r) \tag{6}$$

for minerals and organic liquids, with $V^{o}_{T_r,P_r}$ representing the standard molal volume of the species at the reference temperature and pressure of 25°C and 1 bar. Adopting for gases a standard state of unit fugacity of the pure hypothetical ideal gas at 1 bar and any temperature requires that:

$$V^{o} = 0 \tag{7}$$

for gases at all temperatures and pressures [6]. Finally, the partial molal equivalent of Equation (4) for aqueous species which may be written as:

$$\begin{aligned} \overline{G}^{\circ}_{T,P} - \overline{G}^{\circ}_{T_r,P_r} = & - \overline{S}^{\circ}_{T_r,P_r} (T - T_r) \\ & + \int_{T_r}^{T} \overline{C}^{\circ}_{P_r} dT - T \int_{T_r}^{T} \overline{C}^{\circ}_{P_r} d \ln T + \int_{P_r}^{P} \overline{V}^{\circ} dP \end{aligned} \tag{8}$$

is evaluated by taking account of the revised Helgeson-Kirkham-Flowers equations of state for the standard partial molal heat capacity and standard partial molal volume at the temperature and pressure of interest, which are given by [12]:

$$\begin{aligned} \overline{C}^{\circ}_{P_r} = & c_1 + \frac{c_2}{(T-\theta)^2} - \left[\frac{2T}{(T-\theta)^3}\right] \times \left[a_3 (P - P_r) + a_4 \ln\left(\frac{\Psi + P}{\Psi + P_r}\right)\right] \\ & + \omega T X + 2TY \left(\frac{\partial \omega}{\partial T}\right)_P - T \left(\frac{1}{\varepsilon - 1}\right)\left(\frac{\partial^2 \omega}{\partial T^2}\right)_P \end{aligned} \tag{9}$$

and:

$$\begin{aligned} \overline{V}^{\circ} = & a_1 + a_2 \left(\frac{1}{\Psi + P}\right) \\ & + \left[a_3 + a_4 \left(\frac{1}{\Psi + P}\right)\right]\left(\frac{1}{T - \theta}\right) - \omega Q + \left(\frac{1}{\varepsilon} - 1\right)\left(\frac{\partial \omega}{\partial P}\right)_T \end{aligned} \tag{10}$$

where a_1, a_2, a_3, a_4, c_1, c_2, and ω represent species-dependent equation of state parameters, ψ and θ designate solvent-dependent parameters equal to 2600 bar and 228 K, ε is the dielectric constant of H_2O, and Q, X, and Y refer to the Born functions. The equations summarized above can be solved with the aid of the SUPCRT92 computer program [13], together with thermodynamic properties and parameters for minerals, gases, aqueous species, and liquid hydrocarbons and organic sulfur compounds [7-9, 14, 15]. The thermodynamic properties at 25°C and 1 bar, heat capacity coefficients, and transition properties at 1 bar for elemental sulfur are the following [16]:

ΔG^{o}_{f} [a]	ΔH^{o}_{f} [a]	S^{o} [b]	V^{o} [c]
0	0	7.6	15.511

a [b]	b [d]	c [e]	T_{t,P_r} [f]	$\Delta H^{o}_{t,P_r}$ [a]	$\Delta V^{o}_{t,P_r}$ [c]
3.58	0.00624	0	368.6	86	0.979
3.56	0.00696	0	392	410	1.137
5.4	0.005	0	718	–	–

[a] cal mol^{-1}; [b] cal mol^{-1}K^{-1}; [c] cm^{3}mol^{-1}; [d] cal mol^{-1}K^{-2}; [e] cal K mol^{-1}; [f] K.

2 FORMATION WATER CHEMISTRY IN CARBONATE RESERVOIRS

Thermodynamic calculations indicate that most formation waters produced from carbonate reservoirs are close to equilibrium with respect to calcite and dolomite, but not anhydrite [17-19]. This is illustrated in Figure 1, where values of the saturation index computed in the manner described below with the EQUIL program [20] for these three minerals have been plotted as a function of reservoir temperature. The symbols correspond to formation waters produced from Jurassic reservoirs of the Paris Basin [17] and the North Sea [18], as well as Devonian rocks from the Alberta Basin [19]. Only those waters for which the electric neutrality was respected within:

$$\sum m_i z_i = \pm 0.1 \tag{11}$$

where m_i and z_i stand for the molality and charge of the ith ionic species, were considered in the calculations. The saturation index Ω is defined by:

$$\Omega = \log \frac{Q_r}{K_r} \tag{12}$$

where Q_r denotes the ion activity product and K_r represents the equilibrium constant for the rth reaction. The ion activity product is in this case defined by the product of the aqueous activities of the constitutive ions of the mineral for which the saturation test is performed according to:

$$Q_r = \prod_i a_i^{n_i} \tag{13}$$

where a_i and n_i stand for the activity and stoichiometric coefficient of the ith ionic species, respectively. The activity a_i of an aqueous species is defined by:

$$a_i = \gamma_i m_i \tag{14}$$

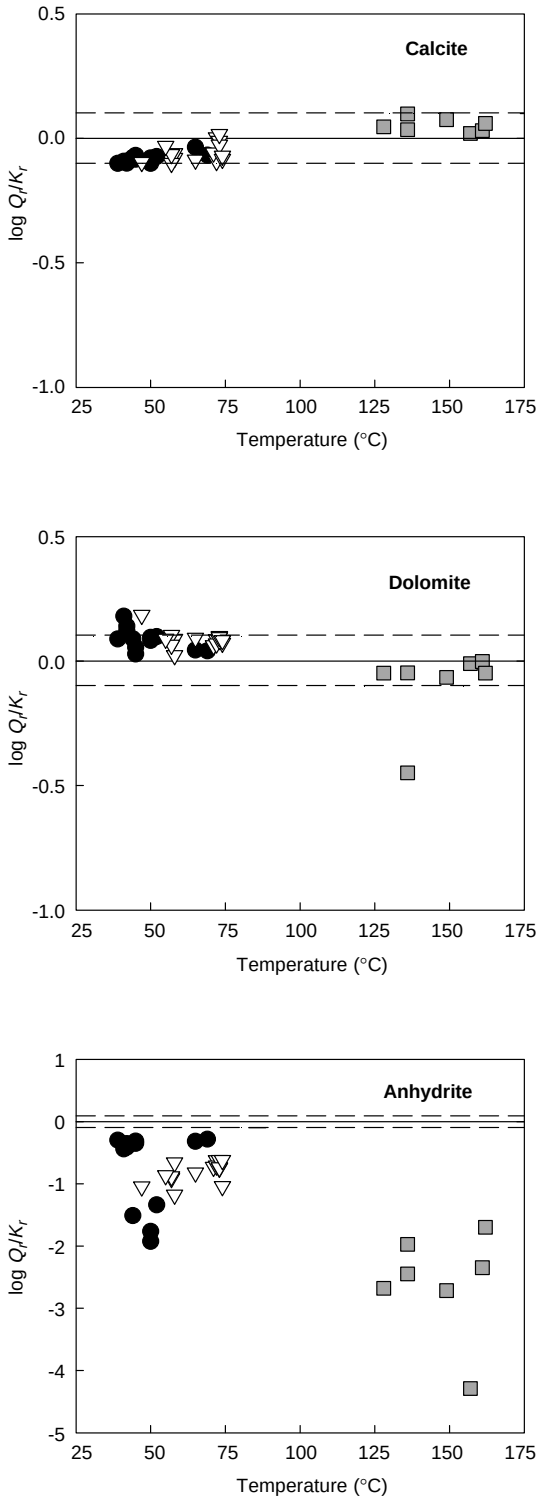

Figure 1

Saturation index for calcite, dolomite, and anhydrite as a function of temperature. The symbols correspond to formation waters of the Alberta Basin (●), the Paris Basin (∇), and the North Sea (■). The solid and dashed lines indicate solution-mineral equilibrium and departures of ± 0.1 log unit from this equilibirum, respectively – see text.

where γ_i and m_i designate the activity coefficient and molality of the *i*th species in the formation water. Activity coefficients of ionic species are computed by the EQUIL program using the Debye-Hückel equation modified by Helgeson [21].

According to a procedure described elsewhere [19], the pH values of the fluids were first adjusted to bring calcite to within ± 0.1 log unit from equilibrium. This pH adjustment is based on the hypothesis that pH values measured at the surface are somewhat different from the actual values at depth, as well as on the observation that calcite is usually the most abundant mineral in carbonate reservoirs. These recalculated pH values were in all cases less than a unit lower than the corresponding surface values. In addition, the pH adjustment resulted in 29 formation waters of the 34 considered in the calculations to be in equilibrium with respect to dolomite within ± 0.1 log unit (dashed lines in *Fig. 1*).

When sulfate and sulfide concentrations were reported separately for the formation waters [17, 19], the saturation calculations for anhydrite were constrained by specifying oxygen fugacity ($f_{O_{2(g)}}$) values at each temperature which would correctly reproduce the sulfate and sulfide concentrations in the fluid at the adjusted pH value according to the reaction:

$$SO_4^{2-} + 2\ H^+ = H_2S_{(aq)} + 2\ O_{2(g)} \qquad (15)$$

It can be seen in Figure 1 that all formation waters are undersaturated with respect to anhydrite, in particular the higher temperature waters from the North Sea in which the sulfate concentrations are extremely low (0.1-1.1 10^{-3} mol). The oxygen fugacity values constrained by the sulfate-sulfide equilibrium have been plotted as a function of temperature in Figure 2, and compared to those computed for the hematite-magnetite (HM-MT) and pyrrhotite-pyrite-magnetite (PO-PY-MT) buffers, both of which are representative of the oxidation-reduction conditions prevailing in sedimentary basins [6, 22]. These mineral buffers correspond to the reactions:

$$3\ Fe_2O_3 = 2\ Fe_3O_4 + 0.5\ O_{2(g)} \qquad (16)$$

for the hematite-magnetite buffer, and:

$$6\ FeS + 2\ O_{2(g)} = 3\ FeS_2 + Fe_3O_4 \qquad (17)$$

for the pyrrhotite-pyrite-magnetite buffer, respectively. The temperature-log $f_{O_{2(g)}}$ curves corresponding to Reactions (16) and (17) were computed with the SUPCRT92 software [13] along the liquid-vapor saturation curve for the system H_2O. Although the oxygen fugacity values computed assuming equilibrium between sulfate and sulfide species represent a smooth distribution as a function of temperature and pressure, these values plot more than 3 log units above the hematite-magnetite assemblage. It has been demonstrated that the oxygen fugacity values in calcite-bearing reservoirs

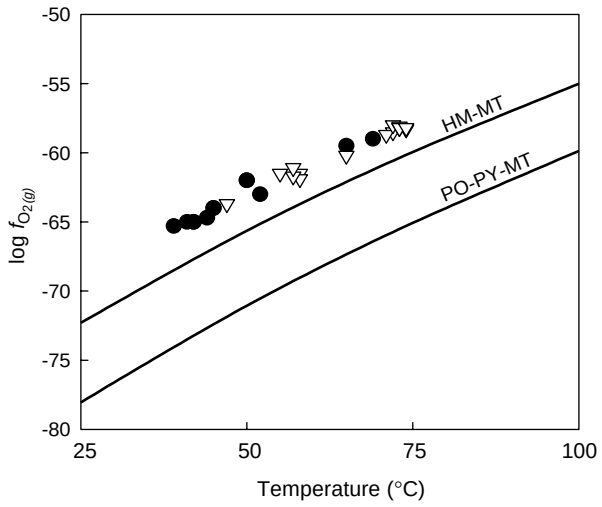

Figure 2

Logarithm of the fugacity of $O_{2(g)}$ as a function of temperature. The symbols represent log $f_{O_{2(g)}}$ values computed assuming equilibrium between sulfate and sulfide aqueous species in the formation waters of the Alberta Basin (●) and the Paris Basin (∇). The curves correspond to log $f_{O_{2(g)}}$ values set by the hematite-magnetite (HM-MT) and pyrrhotite-pyrite-magnetite (PO-PY-MT) buffers.

represent metastable equilibrium states between the heavier hydrocarbons in crude oil (*i.e.* with carbon numbers ≥ 6-15), aqueous organic (*e.g.* carboxylate anions) and inorganic carbon-bearing species, and calcite, and that these values fall within the range defined by the hematite-magnetite and pyrrhotite-pyrite-magnetite assemblages [6, 22]. The reason for these higher oxygen fugacity values is unclear, but may be due to inconsistencies between thermodynamic data in the EQUIL and SUPCRT92 databases.

The fact that anhydrite is not at equilibrium with formation waters in diagenetic environments is well known in carbonate reservoirs associated with appreciable concentrations of hydrogen sulfide (H_2S). As a result, elemental sulfur may form in such reservoirs [23, 24] according to the reaction:

$$CaSO_4 + 3\ H_2S_{(aq)} + 2\ H^+ = 4\ S_{(c\ or\ l)} + 4\ H_2O + Ca^{2+} \quad (18)$$

A diagram showing the stability domains of elemental sulfur, anhydrite, and calcite at 50°C and 1 bar is depicted in Figure 3. The reactions for the lines corresponding to coexisting calcite and anhydrite, and coexisting calcite and elemental sulfur are:

$$CaSO_4 + 4\ CO_{2(g)} + 3\ Ca^{2+} + 4\ H_2O = 4\ CaCO_3 + H_2S_{(aq)} + 6\ H^+ + 2\ O_{2(g)} \quad (19)$$

and:

$$CaCO_3 + 2\ H^+ + H_2S_{(aq)} + 0.5\ O_{2(g)} = Ca^{2+} + CO_{2(g)} + S_{(c\ or\ l)} + 2\ H_2O \quad (20)$$

respectively. The invariant point in Figure 3 corresponds to the reaction:

$$CaSO_4 + 2\ H_2S_{(aq)} + CO_{2(g)} = 3\ S_{(c\ or\ l)} + CaCO_3 + 2\ H_2O + 0.5\ O_{2(g)} \quad (21)$$

The equation of the three lines were obtained from equilibrium constants calculated with the SUPCRT92 software [13] and logarithmic expressions of the law of mass action for Reactions (18)-(20), which can be written as:

$$\log K_{(18)} = \left(a_{Ca^{2+}_{(aq)}} \Big/ a^2_{H^+_{(aq)}}\right) - 3 \log a_{H_2S_{(g)}} \quad (22)$$

$$\log K_{(19)} = \log a_{H_2S_{(aq)}} + 2\ \log f_{O_{2(g)}} - 3\ \log \left(a_{Ca^{2+}_{(aq)}} \Big/ a^2_{H^+_{(aq)}}\right) \quad (23)$$

and:

$$\log K_{(20)} = \log \left(a_{Ca^{2+}_{(aq)}} \Big/ a^2_{H^+_{(aq)}}\right) - \log\ a_{H_2S_{(aq)}} - 0.5\ \log f_{O_{2(g)}} \quad (24)$$

assuming a carbon dioxide fugacity $f_{CO_{2(g)}}$ = 1 bar and an oxygen fugacity $f_{O_{2(g)}}$ value buffered by Reaction (17). It can be seen in Figure 3 that all of the formation waters from the Paris Basin and Alberta Basin plot inside the stability field of calcite. However, it can also be deduced from that figure that the injection of H_2S gas in a carbonate reservoir will tend to move the fluid composition towards the stability field of elemental sulfur. It should be noted that Reactions (18) and (20) both permit the sequestration of H_2S under the form of elemental sulfur. Other possible controls on H_2S partial pressures in carbonate reservoirs are the precipitation

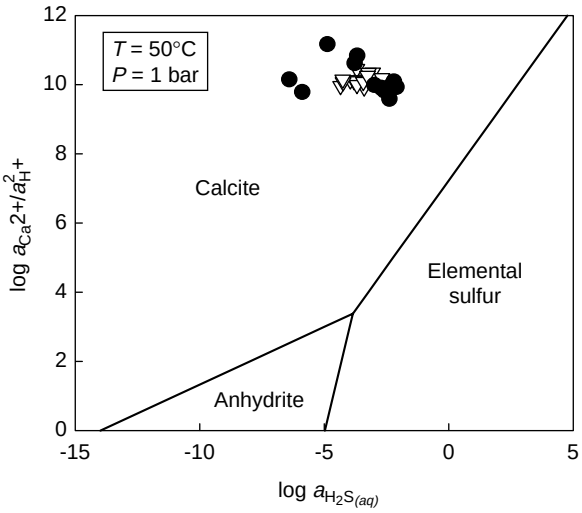

Figure 3

Activity diagram depicting the stability fields of calcite, anhydrite, and elemental sulfur at 50°C and 1 bar. The symbols correspond to formation waters of the Alberta Basin (●) and the Paris Basin (∇).

of metal sulfides and the formation of organic sulfur compounds through sulfurization of residual hydrocarbons in the depleted reservoirs. Precipitation of metal sulfides (*e.g.* pyrite) is a limited process in carbonate reservoirs due to the limited availability of metal ions [24, 25]. Limited amounts of pyrite and marcasite have been formed in the carbonate reservoirs of the Nisku formation [24] as products of bacterial and thermochemical sulfate reduction. The formation of metal sulfides will not be further discussed since metal concentrations have not been reported for the formation waters of the Paris Basin and the North Sea considered in the present study. Petroleum sulfurization reactions leading to the formation of organic sulfur compounds are described in detail below.

3 HIGH H_2S IN PETROLEUM AND NATURAL GAS RESERVOIRS

High concentrations of H_2S gas are encountered in carbonate reservoirs in which thermochemical sulfate reduction has occurred [26-29]. This makes such reservoirs potential natural analogues for geochemical studies related to the sequestration of H_2S in the subsurface. Partial pressures of H_2S ($p_{H_2S_{(g)}}$) as high as ~ 400 bar have been reported in Devonian gas reservoir rocks from the Alberta Basin, Canada [29]. The amount of H_2S gas in these rocks is higher than that of CO_2, and tends to increase with increasing temperature (or depth). To illustrate this dependence of $p_{H_2S_{(g)}}$ with respect to temperature, mole fractions of H_2S ($x_{H_2S_{(g)}}$) reported for the upper Devonian Nisku reservoirs of Alberta [28] have been converted to H_2S partial pressures ($p_{H_2S_{(g)}}$) according to:

$$p_{H_2S_{(g)}} = x_{H_2S_{(g)}} \cdot P \qquad (25)$$

where P is the total pressure, and plotted against temperature in Figure 4. It can be seen in this figure that the values of $p_{H_2S_{(g)}}$ start to increase exponentially with increasing present-day temperatures in the Nisku reservoirs above ~ 110ºC. Also plotted in Figure 4 is the highest partial pressure of H_2S (~ 360 bar at ~ 130°C) reported by Hutcheon [29] which is in agreement with the lower temperature data and the exponential trend represented by the dashed curve. A similar exponential relationship between H_2S partial pressures and temperature has been proposed for sandstone reservoirs from the Norwegian Shelf [30]. The partial pressures of H_2S in the Norwegian Shelf and the Alberta Basin are compared in Figure 5 on a log $p_{H_2S_{(g)}}$ *versus* temperature plot. It can be seen in this figure that the values of $p_{H_2S_{(g)}}$ in clastic reservoirs are lower by several orders of magnitude than those observed in carbonate rocks. This difference is classically interpreted as reflecting the lack of available iron in carbonate reservoirs to buffer the $p_{H_2S_{(g)}}$ values by forming iron sulfides [26, 29]. In fact, it has been shown that the values of $p_{H_2S_{(g)}}$ in the clastic reservoirs of the Norwegian Shelf were most probably controlled by an iron sulfide-iron carbonate assemblage [22], for which an equilibrium relation may be written as:

$$FeS_2 + CO_{2(g)} + H_{2(g)} + H_2O_{(l)} = FeCO_3 + 2\ H_2S_{(g)} \qquad (26)$$

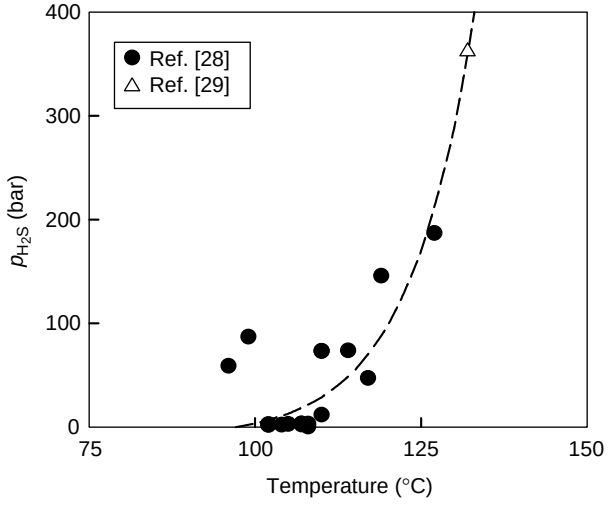

Figure 4

Partial pressure of H_2S as a function of temperature. The symbols correspond to values reported for carbonate reservoirs from the Alberta Basin. The dashed curve has been drawn to illustrate the exponential increase of pH_2S with increasing temperature.

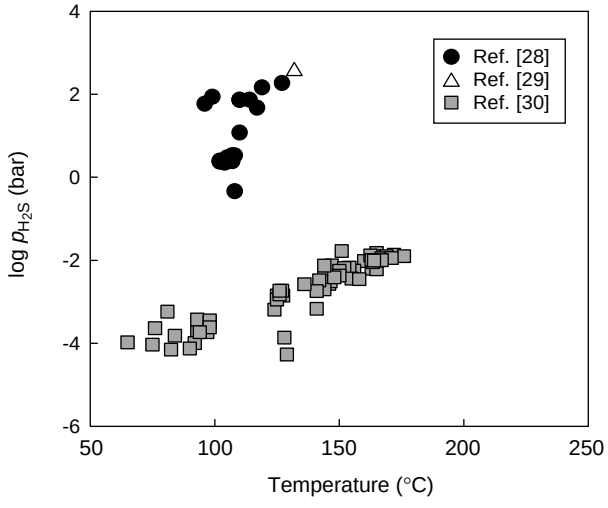

Figure 5

Logarithm of the partial pressure of H_2S as a function of temperature. The symbols correspond to values reported for carbonate reservoirs from the Alberta Basin (● and Δ) and clastic reservoirs from the North Sea (■).

where FeS_2 and $FeCO_3$ represent the minerals pyrite and siderite, $H_2O_{(l)}$ stands for liquid water, and $CO_{2(g)}$, $H_{2(g)}$, and $H_2S_{(g)}$ denote CO_2, H_2, and H_2S in the gas state, respectively. It has also been demonstrated that metastable equilibrium states between hydrocarbons, organic sulfur compounds and H_2S gas could establish in hydrocarbon reservoirs [31]. The possibility that such metastable equilibrium states could control the partial pressures of H_2S in carbonate reservoirs is evaluated below.

4 METASTABLE EQUILIBRIUM STATES AMONG HYDROCARBONS, H_2S, NATIVE SULFUR, AND ORGANIC SULFUR COMPOUNDS

Organic sulfur compounds first form during early diagenetic processes through reactions between bacterially produced hydrogen sulfide and carbon-carbon double bonds or oxygen-bearing functional groups of the biological precursors of sedimentary organic matter [32]. These reactions result in the formation of sulfur-rich kerogens, and the subsequent generation of sulfur-rich crude oils from these kerogens. However, there is ample experimental and field evidence that H_2S, elemental sulfur, and hydrocarbons equally react in petroleum reservoirs to produce organic sulfur compounds. Sulfurization of petroleum in carbonate reservoirs through reactions between hydrocarbons and elemental sulfur has been abundantly discussed in the Russian literature [33, and references therein]. Thiols, sulfides and disulfides have been experimentally produced by reacting low molecular weight hydrocarbons (*e.g. n*-heptane and cyclohexane) with elemental sulfur at temperatures as low as 50°C [33]. Hydrogen sulfide was formed as a by-product in some of these experiments. Similarly, a mixture of C_{18} *n*-2,5-dialkylthiophenes has been produced by reacting *n*-octadecane with elemental sulfur at temperatures between 200 and 250°C [34]. It has also been observed that there was an increase in aromatic sulfur compounds (*e.g.* benzothiophenes) in the Nisku reservoirs of Alberta with increasing H_2S in the gas phase of these reservoirs [28]. Although elemental sulfur may accumulate in petroleum reservoirs as a net product of thermochemical sulfate reduction [25], it should perhaps be pointed out that elemental sulfur and hydrogen sulfide may appear as reactants or products depending on the hydrogen to carbon (H/C) ratios of the hydrocarbons and organic sulfur compounds involved in the multitude of sulfurization reactions that may occur in a petroleum reservoir (see below). In any event, experiments and observations of this kind suggest that reactions involving hydrocarbons, elemental sulfur, and organic sulfur compounds may control H_2S partial pressures in carbonate reservoirs.

Recognizing that carbon atoms in organic compounds have different oxidation states depending on the neighboring atom to which they are bonded [35], one can write oxidation-reduction reactions describing metastable equilibrium states between hydrocarbons, elemental sulfur, organic sulfur compounds and hydrogen sulfide. For example, such reactions can be written for liquid 2,4-dimethylbenzo[*b*]thiophene ($C_{10}H_{10}S_{(l)}$) and *trans*-2-methyl-5-*n*-pentylthiacyclopentane ($C_{10}H_{20}S_{(l)}$) coexisting metastably with liquid *n*-decane ($C_{10}H_{22(l)}$) or *n*-butylbenzene ($C_{10}H_{14(l)}$) as:

$$C_{10}H_{22(l)} + 7\ S_{(c\ or\ l)} = C_{10}H_{10}S_{(l)} + 6\ H_2S_{(g)} \quad (27)$$

$$C_{10}H_{22(l)} + 2\ S_{(c)} = C_{10}H_{20}S_{(l)} + H_2S_{(g)} \quad (28)$$

$$C_{10}H_{14(l)} + 3\ S_{(c\ or\ l)} = C_{10}H_{10}S_{(l)} + 2\ H_2S_{(g)} \quad (29)$$

and:

$$C_{10}H_{14(l)} + 3\ H_2S_{(g)} = C_{10}H_{20}S_{(l)} + 2\ S_{(c\ or\ l)} \quad (30)$$

where $S_{(c\ or\ l)}$ and $H_2S_{(g)}$ stand for crystalline or liquid elemental sulfur and hydrogen sulfide gas, respectively. The two organic sulfur compounds involved in Reactions (27)-(30) have been chosen because alkylthiacyclopentanes and alkylbenzothiophenes are representative of immature and mature crude oils, respectively [32]. Their idealized structures are depicted in Figure 6 along with those of *n*-decane and *n*-butylbenzene.

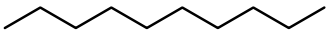

n-decane ($C_{10}H_{22}$)

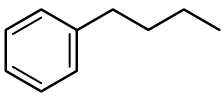

n-butylbenzene ($C_{10}H_{14}$)

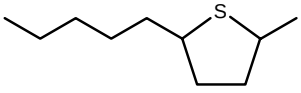

trans-2-methyl-5-pentylthiacyclopentane ($C_{10}H_{20}S$)

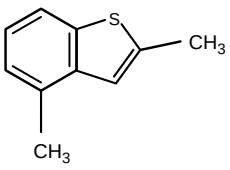

2,4-dimethylbenzo[*b*]thiophene ($C_{10}H_{10}S$)

Figure 6

Idealized structures of the hydrocarbons and organic sulfur compounds considered in the metastable equilibrium state calculations – see text.

Adopting a standard state of unit activity for elemental sulfur at all temperatures and pressures, the corresponding logarithmic expressions of the law of mass action for Reactions (27)-(30) are:

$$\log K_{(27)} = \log \frac{a_{C_{10}H_{10}S_{(l)}}}{a_{C_{10}H_{22(l)}}} + 6 \log f_{H_2S_{(g)}} \quad (31)$$

$$\log K_{(28)} = \log \frac{a_{C_{10}H_{20}S_{(l)}}}{a_{C_{10}H_{22(l)}}} + \log f_{H_2S_{(g)}} \quad (32)$$

$$\log K_{(29)} = \log \frac{a_{C_{10}H_{10}S_{(l)}}}{a_{C_{10}H_{14(l)}}} + 2 \log f_{H_2S_{(g)}} \quad (33)$$

and:

$$\log K_{(30)} = \log \frac{a_{C_{10}H_{20}S_{(l)}}}{a_{C_{10}H_{14(l)}}} - 3 \log f_{H_2S_{(g)}} \quad (34)$$

respectively, where $K_{(27)}$, $K_{(28)}$, $K_{(29)}$, and $K_{(30)}$ are the equilibrium constants for the subscripted reactions, $a_{C_{10}H_{10}S_{(l)}}$, $a_{C_{10}H_{20}S_{(l)}}$, $a_{C_{10}H_{22(l)}}$ and $a_{C_{10}H_{14(l)}}$ stand for the activities of the subscripted species, and $f_{H_2S_{(g)}}$ represent the fugacity of hydrogen sulfide gas. Values of the equilibrium constants for Reactions (27)-(30) have been calculated with the SUPCRT92 software [13] at temperatures and pressures representative of those in the Alberta Basin [28], and used together with Equations (31)-(34) to generate the dashed curves shown in Figure 7. These curves have been drawn for

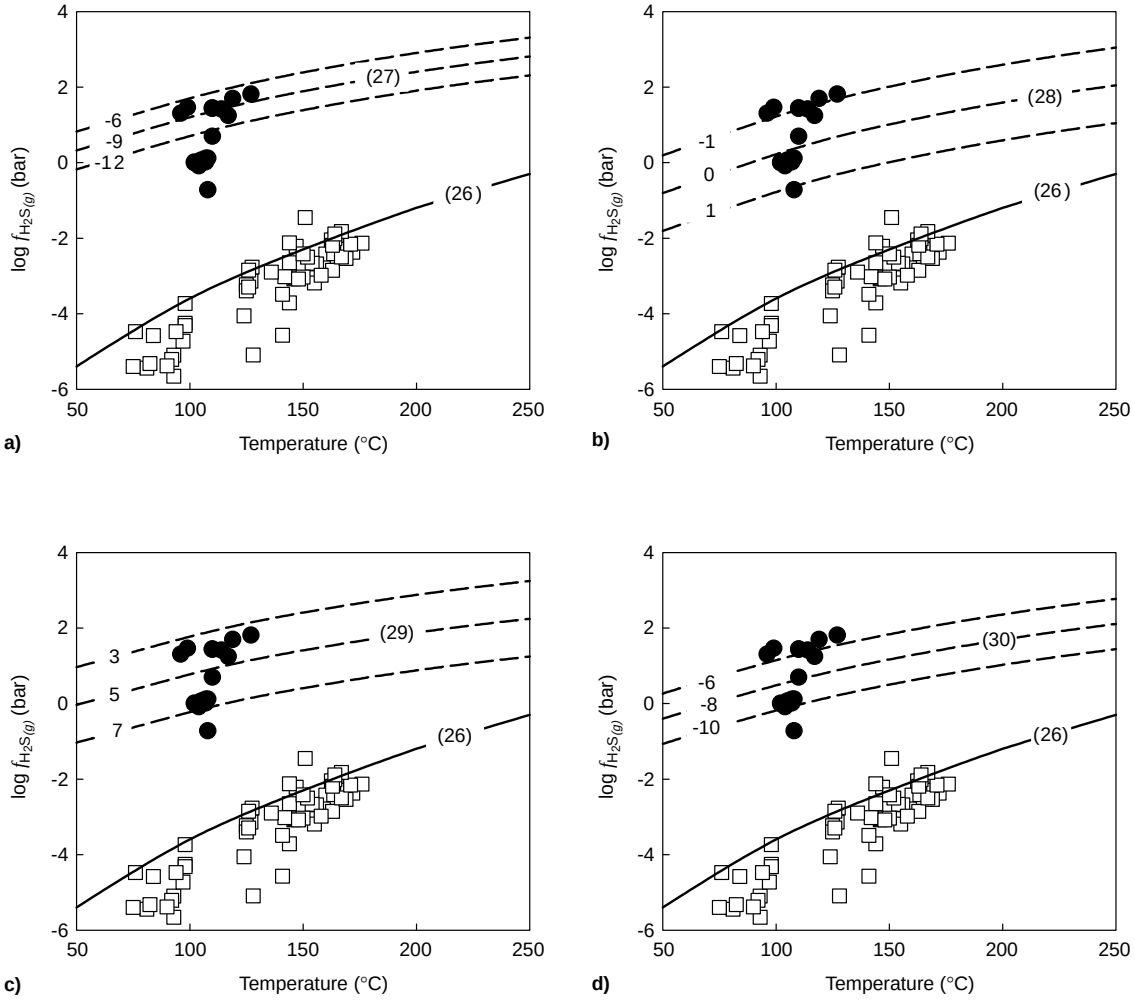

Figure 7

Logarithm of the fugacity of H_2S as a function of temperature. The symbols correspond to values computed from partial pressures of H_2S reported for carbonate reservoirs from the Alberta Basin (●) and clastic reservoirs from the North Sea (□) – see text. The solid curve corresponds to the values fixed by the iron sulfide-iron carbonate assemblage. The dashed curves correspond to values calculated assuming metastable equilibrium states between elemental sulfur, H_2S, and a) *n*-decane and 2,4-dimethylbenzo[*b*]thiophene; b) *n*-decane and *trans*-2-methyl-5-*n*-pentylthiacyclopentane; c) *n*-butylbenzene and 2,4-dimethylbenzo[*b*]thiophene; d) *n*-butylbenzene and *trans*-2-methyl-5-*n*-pentylthiacyclopentane. The numbers between parentheses correspond to Reactions (26)-(30) in the text. The numbers on each curve correspond to different activity ratios of the hydrocarbon and organic sulfur compound in Equations (31)-(34) – see text.

different activity ratios of the hydrocarbon and organic sulfur compound in a given reaction (see caption to *Fig. 7*).

The partial pressures of H_2S ($p_{H_2S_{(g)}}$) shown in Figures 4 and 5 [28, 30] have been converted to their fugacity counterparts ($f_{H_2S_{(g)}}$) according to:

$$f_{H_2S_{(g)}} = \varphi_{H_2S_{(g)}} \cdot p_{H_2S_{(g)}} \quad (35)$$

where $\varphi_{H_2S(g)}$ stands for the fugacity coefficient of H_2S gas, which was evaluated in the present study from the Peng-Robinson equation of state [36]:

$$P = \frac{RT}{V-b} - \frac{a(T)}{V(V+b) + b(V-b)} \quad (36)$$

where V stands for the molal volume of the gas mixture, b is a constant representing a correction for the repulsion between molecules and is defined by:

$$b = 0.07780 \frac{R\,T_c}{P_c} \quad (37)$$

and $a(T)$ is a temperature-dependent constant representing intermolecular attraction forces, which is equal to:

$$a(T) = 0.45724 \frac{R^2\,T_c^2}{P_c} \left[1 + \kappa \left(1 - \left(\frac{T}{T_c}\right)^{1/2}\right)\right]^2 \quad (38)$$

where T_c and P_c designate the critical temperature and pressure, respectively, and κ is a constant characteristic for each gas which is defined by [36]:

$$\kappa = 0.37464 + 1.54226\,\omega - 0.26992\,\omega^2 \quad (39)$$

where ω is the acentric factor. The $a(T)$ and b parameters in Equation (36) were calculated assuming a CO_2-H_2S binary mixture and the usual mixing rules [37]. The fugacity coefficient for H_2S in the mixture is obtained from [37]:

$$\ln \varphi_{H_2S_{(g)}} = \frac{b_{H_2S}}{b}\left(\frac{PV}{RT} - 1\right) - \ln \frac{P(V-b)}{RT} - \frac{a(T)}{2\sqrt{2}\,bRT} \left[\frac{2\left(z_{CO_{2(g)}} a_{CO_2-H_2S} + z_{H_2S_{(g)}} a_{H_2S}\right)}{a(T)} - \frac{b_{H_2S}}{b}\right] \ln \frac{V + (1+\sqrt{2})b}{V + (1-\sqrt{2})b} \quad (40)$$

where $z_{CO_2(g)}$ and $z_{H_2S(g)}$ are the mole fractions of CO_2 and H_2S in the gas mixture.

The solid curve shown in Figure 7 represents the H_2S fugacity fixed by the pyrite-iron carbonate assemblage for the clastic reservoirs from the Norwegian shelf [22]. It can be seen in Figure 7 that all but one of the fugacities of H_2S in the Alberta Basin carbonate reservoirs fall within the range defined by Reactions (27)-(30) and the activity ratios indicated on the different curves. Note that the standard molal thermodynamic properties of organic compounds are a nearly linear function of carbon number for homologous series of compounds [8, 9]. Therefore, metastable equilibrium curves calculated for *n*-alkanes, *n*-alkylbenzenes, and *n*-alkylthiacyclopentanes with higher or lower carbon numbers would coincide nearly exactly with the curves shown for *n*-decane, *n*-butylbenzene, and *trans*-2-methyl-5-*n*-pentylthiacyclopentane in Figure 7. Similarly, many other metastable equilibrium states involving hydrocarbons and organic sulfur compounds with different nominal oxidation states are consistent with the range of H_2S partial pressures reported for the Nisku and other carbonate reservoirs in which thermochemical sulfate reduction may have occurred [31]. The important point is that these preliminary calculations suggest that in the absence of detrital iron, metastable equilibrium states between hydrocarbons, hydrogen sulfide, elemental sulfur and organic sulfur compounds may control the partial pressures of H_2S in carbonate reservoirs at values which are 4 to 6 orders of magnitude higher than those encountered in sandstone reservoirs.

CONCLUSION

As part of a research project on the chemical and mineralogical consequences of injecting CO_2-H_2S gas mixtures in geological formations, the water-gas-rock-hydrocarbon reactions involving sulfur in carbonate reservoirs have been analyzed from a thermodynamic point of view. The calculations indicate that increasing the partial pressure of H_2S in a carbonate reservoir, thereby increasing the aqueous activity of H_2S in the formation water, will favor the formation of elemental sulfur. This constitutes a potential sequestration reaction for H_2S.

Considering carbonate reservoirs in which thermochemical sulfate reduction has occurred as natural analogues for the sequestration of H_2S suggests that the partial pressures of H_2S in these reservoirs may be controlled by metastable equilibrium states between hydrocarbons, organic sulfur compounds and elemental sulfur. Changing the fugacity of H_2S in carbonate reservoirs could possibly affect these metastable equilibrium states. Although the kinetics of sulfurization reactions is not known, these reactions may consume or produce H_2S depending on the H/C ratios of the hydrocarbons and organic sulfur compounds involved in the sulfurization reactions. Future research will be aimed at quantifying these reactions by performing mass transfer and Gibbs free energy minimization calculations to confirm the preliminary calculations presented in this communication.

ACKNOWLEDGEMENTS

The authors are grateful to Étienne Brosse for encouraging them to submit this paper. Constructive comments by two

anonymous reviewers are sincerely appreciated. This study was carried out with financial support from *Total* (contract TOTAL DGEP/TDO/CA/ACOMS CT No. 13444).

REFERENCES

1 Hansen, J.E., Sato, M., Lacis, A., Ruedy, R., Tegen, I. and Matthews, E. (1998) Climate Forcings in the Industrial Era. *Proceedings of the National Academy of Sciences*, **95**, 22, 12753-12758.

2 Lackner, K.S. (2003) A Guide to CO_2 Sequestration. *Science*, **300**, 5626, 1677-1678.

3 Gunter, W.G., Wiwchar, B., and Perkins, E.H. (1997) Aquifer Disposal of CO_2-Rich Greenhouse Gases: Extension of the Time Scale of Experiment for CO_2-Sequestering Reactions by Geochemical Modelling. *Mineralogy and Petrology*, **59**, 1-2, 121-140.

4 Gunter, W.G., Perkins, E.H., and Hutcheon, I. (2000) Aquifer Disposal of Acid Gases: Modelling of Water-Rock Reactions for Trapping of Acid Wastes. *Applied Geochemistry*, **15**, 8, 1085-1095.

5 Xu, T., Apps, J.A., and Pruess, K. (2004) Numerical Simulation of CO_2 Disposal by Mineral Trapping in Deep Aquifers. *Applied Geochemistry*, **19**, 6, 917-936.

6 Helgeson, H.C., Knox, A.M., Owens, C.E. and Shock, E.L. (1993) Petroleum, Oil Field Waters, and Authigenic Mineral Assemblages: Are they in Metastable Equilibrium in Hydrocarbon Reservoirs? *Geochimica Cosmochimica Acta*, **57**, 14, 3295-3339.

7 Helgeson, H.C., Delany, J.M., Nesbitt, H.W. and Bird, D.K. (1978) Summary and Critique of the Thermodynamic Properties of Rock-Forming Minerals. *American Journal of Science*, **278-A**, 1-229.

8 Helgeson, H.C., Owens, C.E., Knox, A.M. and Richard, L. (1998) Calculation of the Standard Molal Thermodynamic Properties of Crystalline, Liquid, and Gas Organic Molecules at high temperatures and pressures. *Geochimica Cosmochimica Acta*, **62**, 6, 985-1081.

9 Richard, L. (2001) Calculation of the Standard Molal Thermodynamic Properties as a Function of Temperature and Pressure of some Geochemically Important Organic Sulfur Compounds. *Geochimica Cosmochimica Acta*, **65**, 21, 3827-3877.

10 Maier, C.G. and Kelley, K.K. (1932) An Equation for the Representation of High Temperature Heat-Content Data. *Journal of the American Chemical Society*, **54**, 8, 3243-3246.

11 Richard, L. and Helgeson, H.C. (2004) *Calculation of the Standard Molal Volumes of Crystalline and Liquid Organic Compounds as a Function of Temperature and Pressure* (in preparation).

12 Tanger, J.C. and Helgeson, H.C. (1988) Calculation of the Thermodynamic and Transport Properties of Aqueous Species at High Pressures and Temperatures: Revised Equations of State for the Standard Partial Molal Properties of Ions and Electrolytes. *American Journal of Science*, **288**, 1, 19-98.

13 Johnson, J.W., Oelkers, E.H. and Helgeson, H.C. (1992) SUPCRT92: A Software Package for Calculating the Standard Molal Thermodynamic Properties of Minerals, Gases, Aqueous Species, and Reactions from 1 to 5000 bar and 0 to 1000ºC. *Computers and Geosciences*, **18**, 7, 899-947.

14 Shock, E.L. and Helgeson, H.C. (1988) Calculation of the Thermodynamic and Transport Properties of Aqueous Species at High Pressures and Temperatures: Correlation Algorithms for Ionic Species and Equation of State Predictions to 5 kb and 1000°C. *Geochimica Cosmochimica Acta*, **52**, 8, 2009-2036.

15 Shock, E.L., Helgeson, H.C., and Sverjensky, D.A. (1989) Calculation of the Thermodynamic and Transport Properties of Aqueous Species at High Pressures and Temperatures: Standard Partial Molal Properties of Inorganic Neutral Species. *Geochimica Cosmochimica Acta*, **53**, 9, 2157-2183.

16 Gurrieri, S. (1997) Personal Communication.

17 Michard, G. and Bastide, J.P. (1988) Étude géochimique de la nappe du Dogger du Bassin parisien. *Journal of Volcanology and Geothermal Research*, **35**, 1/2, 151-163.

18 Egeberg, P.K. and Aagaard, P. (1989) Origin and Evolution of Formation Waters from Oil Fields on the Norwegian Shelf. *Applied Geochemistry*, **4**, 2, 131-142.

19 Connolly, C.A., Walter, L.M., Baadsgaard, H. and Longstaffe, F.J. (1990) Origin and Evolution of Formation Waters, Alberta Basin, Western Canada Sedimentary Basin. I. Chemistry. *Applied Geochemistry*, **5**, 4, 375-395.

20 Fritz, B. (1981) Étude thermodynamique et modélisation des réactions hydrothermales et diagénétiques. *Mémoire des Sciences Géologiques*, **65**.

21 Helgeson, H.C. (1969) Thermodynamics of Hydrothermal Systems at Elevated Temperatures and Pressures. *American Journal of Science*, **267**, 7, 729-804.

22 Aagaard, P., Jahren, J.S. and Ehrenberg, S.N. (2001) H_2S-Controlling Reactions in Clastic Hydrocarbon Reservoirs from the Norwegian Shelf and US Gulf Coast. In: *Water-Rock Interaction 2001*, Cidu R. (ed.), Swets & Zeitlinger, Lisse, 129-132.

23 Heydari, E. (1997) The Role of Burial Diagenesis in Hydrocarbon Destruction and H_2S Accumulation, Upper Jurassic Smackover Formation, Black Creek Field, Mississippi. *Bulletin of the American Association of Petroleum Geologists*, **81**, 1, 26-45.

24 Riciputi, L.R., Cole, D.R. and Machel, H.G. (1996) Sulfide Formation in Reservoir Carbonates of the Devonian Nisku Formation, Alberta, Canada: An ion microprobe study. *Geochimica et Cosmochimica Acta*, **60**, 2, 325-336.

25 Machel, H.G. (2001) Bacterial and Thermochemical Sulfate Reduction in Diagenetic Settings – Old and New Insights. *Sedimentary Geology*, **140**, 1/2, 143-175.

26 Orr, W.L. (1977) Geologic and Geochemical Controls on the Distribution of Hydrogen Sulfide in Natural Gas. In: *Advances in Organic Geochemistry 1975*, Campos, R., and Goñi, J. (eds.), Empresa Nacional Adaro De Investigaciones Mineras, Madrid, 571-597.

27 Worden, R.H., Smalley, P.C. and Oxtoby, N.H. (1995) Gas Souring by Thermochemical Sulfate Reduction at 140°C. *Bulletin of the American Association of Petroleum Geologists*, **79**, 6, 854-863.

28 Manzano, B.K., Fowler, M.G. and Machel, H.G. (1997) The Influence of Thermochemical Sulfate Reduction on Hydrocarbon Composition in Nisku Reservoirs, Brazeau River Area, Alberta, Canada. *Organic Geochemistry*, **27**, 7/8, 507-521.

29 Hutcheon, I. (1999) Controls on the Distribution of Non-Hydrocarbon Gases in the Alberta Basin. *Bulletin of Canadian Petroleum Geology*, **47**, 4, 573-593.

30 Håland, K., Barrufet, M.A., Rønningsen, H.P. and Meisingset, K.K. (1999) An Empirical Correlation between Reservoir Temperature and the Concentration of Hydrogen Sulfide. *Proceedings SPE International Symposium on Oilfield Chemistry*, 589-596.

31 Richard, L. and Helgeson, H.C. (2001) Thermodynamic Calculation of the Distribution of Organic Sulfur Compounds in Crude Oil as a Function of Temperature, Pressure, and H_2S Fugacity. In: *Water-Rock Interaction 2001*, Cidu R. (ed.), Swets & Zeitlinger, Lisse, 333-335.

32 Orr, W.L., and Sinninghe Damsté, J.S. (1990) Geochemistry of Sulfur in Petroleum Systems. In: *Geochemistry of Sulfur in Fossil Fuels*, Orr W.L. and White C.M. (eds.), American Chemical Society Symposium Series, 429, American Chemical Society, 2-29.

33 Valitov, N.B. and Valitov, R.B. (1975) The Role of Temperature in Formation of Sulfur-Bearing Petroleums and Catagenetic Hydrogen Sulfide in Carbonate Reservoirs (experimental investigations). *Geochemistry International*, **12**, 5, 73-81.

34 Schmid, J.C., Connan, J. and Albrecht, P. (1987) Occurrence and Geochemical Significance of Long-Chain Dialkylthiacyclopentanes. *Nature*, **329**, 6134, 54-56.

35 Helgeson, H.C. (1991) Organic/Inorganic Reactions in Metamorphic Processes. *Canadian Mineralogist*, **29**, 4, 707-739.

36 Peng, D.Y. and Robinson, D.B. (1976) A New Two-Constant Equation of State. *Industrial and Engineering Chemistry Fundamentals*, **15**, 1, 59-64.

37 Prausnitz, J.M., Lichtenthaler R.N. and de Azevedo E.G. (1986) *Molecular Thermodynamics of Fluid-Phase Equilibria*, 2nd Edition, Prentice-Hall.

Final manuscript received in January 2005